



Definition of sanitary boundaries to prevent ISAv spread between salmon farms in southern Chile based on numerical simulations of currents



Gonzalo Olivares ^a, H.H. Sepúlveda ^{b, *}, B. Yannicelli ^{c, d, e}

^a *i-mar Research Center, University of Los Lagos, Puerto Montt, Chile*

^b *Geophysics Department, University of Concepcion, Barrio Universitario s/n, Casilla 160–C, Concepcion, Chile*

^c *Centro de Estudios Avanzados en Zonas Áridas, Raul Bitran 1305, La Serena, Chile*

^d *Facultad de Cs del Mar y Núcleo Milenio Ecology and Sustainable Management of Oceanic Islands, Universidad Católica del Norte, Larrondo 1281, Coquimbo, Chile*

^e *CURE Rocha, Universidad de la República, Ruta 9 con 15, Uruguay*

ARTICLE INFO

Article history:

Received 17 March 2014

Accepted 19 February 2015

Available online 28 February 2015

Keywords:

sanitary boundaries

ISAv

Atlantic Salmon

spread

numerical model

Chile

ABSTRACT

The infectious Salmon Anemia virus (ISAv) is a pathogen that mainly affects the Atlantic Salmon (*Salmo salar*). It was detected in Norway in 1984 and in June 2007 appeared in Chile, producing a drop of more than 30% in the country's production level. It is expected that with certain regularity, outbreaks will continue to appear in Chile without the need of reintroducing the virus from foreign countries. We present a numerical study of the influence of winds and tides in the dispersion of lagrangian particles to simulate the transport of ISAv in the Aysen region, in southern Chile. This study combines the use of numerical models of the ocean and atmosphere, lagrangian tracking and biological aspects of ISAv infections. As in previous results, a wider dispersion of ISAv was observed during spring tides. Temporal changes in wind significantly modified the transport of viral particles from an infected center. Under similar forcing conditions, the areas of risk associated to culture sites separated by a few kilometers could be very different. Our main results remark the importance of the use of a detailed knowledge of hydrographic and atmospheric circulation in the definition of boundaries for sanitary management areas. We suggest that a methodology similar to the one presented in this study should be considered to define sanitary strategies to minimize the occurrence of native outbreaks of ISAv.

© 2015 Elsevier Ltd. All rights reserved.

1. Introduction

The Infectious Salmon Anemia virus (ISAv) is a pathogen that mainly affects the Atlantic Salmon (*Salmo salar*). Since it was first diagnosed in 1984 in Norway, the ISAv has provoked epizootics in Scotland, Faroe Islands, the east coast of Canada and United States of America. In Chile, the first outbreak was detected in June 2007 and by November 2008 the virus had already spread along 500 km of coastline between 41.5 S and 46.5 S, affecting more than 60% of the country's salmon farms (Katz et al., 2011). One factor that complicates the control of the disease is the genetic variability in the virus. Different strains of ISAv can exist in a fish population, and even within the same fish, each one characterized by different degrees of virulence (Mjaaland et al., 2005; Ritchie et al., 2009). In

Norway, where high prevalence of non-virulent strains of ISAv is commonly found (Raynard et al., 2001; Ritchie et al., 2001), the outbreaks have been linked to the mutation of non-virulent strains into virulent ones (Aldrin et al., 2010). In Chile, where sites with high prevalence of the non-virulent HPRO strain have also been found, it is presumed that the initial outbreak of ISAv probably originated from a *in situ* mutation of the Norwegian strain, introduced a couple of years earlier (Kibenge et al., 2009; Vike et al., 2009). The aforementioned constitutes a scenario whereby, with certain regularity, new outbreaks of ISAv would occur, even without the re-introduction of the virus from outside the country. Under these conditions, eradication becomes extremely difficult, and the control of ISAv in Chile must include a strategy to effectively isolate spontaneous, and unpredictable, outbreaks of the disease (Vike et al., 2009).

The principal mechanism by which fish are infected involves the entry of ISAv through the gills (Totland et al., 1996; Mikalsen et al., 2001). This is possible because the infected fish start to shed viral

* Corresponding author.

E-mail addresses: g.olivares@ulagos.cl (G. Olivares), andres@dgeo.udec.cl (H.H. Sepúlveda), beatriz.yannicelli@ceaza.cl (B. Yannicelli).

particles in detectable quantities 7 days after the infection has occurred, increasing to massive amounts a few days prior to the fish death (Gregory et al., 2009). Since the particles shed into the sea water maintain their infectious capacity for more than 20 h (Nylund et al., 1994), the disease can spread not only from one cage to another within a salmon farm, but also between farms separated by kilometers (Lyngstad et al., 2008). Operations like the transport of fish, fish remains, or water that has contained infected fish, can make this logistic network an efficient way of viral dissemination between farms (Murray et al., 2002; Scheel et al., 2007). On the other hand, the survival of viral particles in the water also permits dispersion of the disease among sites that are hydrodynamically linked (Jarp and Karlsen, 1997; Gustafson et al., 2007a). Although the relative influence of each of these factors on the development of an epizootics is a subject of debate (Aldrin et al., 2010), it is clear that strategies for controlling each process are of a different nature. When an outbreak is dispersed by a shared logistic network, the actual process of pathogen transport can be controlled. In contrast, in current-based dispersion, because marine currents cannot be changed, the only option left is to modify the location of farms from which ISAv is released, e.g. setting distances between them that are larger than the distances swept by currents over the duration of the infection period.

With the aim of improving epidemiological control throughout the entire fjord zone of southern Chile, the Chilean Fisheries Agency (SUBPESCA) established a system of Sanitary Management Areas (SMA). According to present regulations, farms belonging to the same SMA must coordinate production cycles and comply with common rules regarding maximum densities, therapeutic procedures, mortality disposal, and transport of live fish or fish remains. All these measures are attempts to ensure that logistic networks are shared only within a same SMA, and are isolated from the networks used by farms in other SMA. The limits of each SMA were set up before these rules were discussed. At the core of this decision was the assumption that a separation of 11.1 km between farms belonging to different SMA, effectively prevents dispersion of pathogens by currents. This study aims to contribute relevant information to evaluate that assumption, based on numerical simulations of the transport of viral particles forced by a hydrodynamic model.

2. Materials and methods

Water circulation in the fjord region of Chile (Fig. 1) was simulated using the numerical model ROMS (Shchepetkin and MacWilliams, 2005; Penven et al., 2005). ROMS solves primitive equations of fluid dynamics using the hydrostatic approximation, considering a free surface and sigma (terrain-following) vertical coordinates. A 2D version of this model has already been used for studying circulation in the fjords region of Chile (Aiken, 2008), where an adequate representation of sea level in the zone was obtained. To represent propagation of the tides within the region of the austral fjords, ROMS was implemented on the full domain with a spatial resolution of 1.2 km. The results of this simulation were used to force a sub-model, or subdomain, with an approximate resolution of 0.36 km (Fig. 2), using the ROMS2ROMS tool (Mason et al., 2010). Both domains possess 16 vertical levels, distributed so as to provide a more detailed representation of the surface layer. Bathymetry of both domains was generated with GEBCO_08 (IOC et al., 2003), in a 30 s grid (0.83 km) resolution. This bathymetry was compared with charts 7000 and 8000 of the SHOA (Servicio Hidrográfico y Oceanográfico de la Armada de Chile: Hydrographic and Oceanographic Service of the Chilean Navy). Some of the main channels and straits of the zone of interest were corrected by hand.

Given the vast area of the study zone and the limited hydrographic information available, it was decided to initialize the temperature and salinity fields with information taken from the World Ocean Atlas 2001 data base (Conkright et al., 2002). The same information was used to calculate the geostrophic currents at the open boundaries of the model. Tidal forcing was incorporated through the coefficients calculated by the TPX07 model (Egbert and Erofeeva, 2002). Given that the effect of freshwater discharge from the major rivers in the area was not included, it is considered that the model only represents variations in sea level and barotropic currents, as well as the effect of wind on the surface layers. Initial conditions were derived from the WOA data base and a spin-up time of 4 months was prescribed, during this spin-up time the forcing for the December/September scenario was repeated every month. This was done to develop the high resolution features of the velocity fields that were not present in the initial condition.

To describe the climatological atmospheric forcings, information from the COADS (Da Silva et al., 1994) data base was used, interpolating linearly between monthly climatological averages. Temporal variability of atmospheric circulation was represented using the MM5 atmospheric model (Dudhia, 1993). A domain with a spatial resolution of 27 km (Fig. 1), 23 vertical levels and a time step of 70 s was used. Boundary and initial conditions were obtained from reanalysis (Kalnay et al., 1996) for the simulated months. Physical parameterizations selected included the Grell scheme (Grell, 1993) for cumulus parameterization, the planetary boundary layer MRF (Troen and Mahrt, 1986) and the Dudhia ice scheme for cloud microphysics (Dudhia, 1989). Surface sea temperature (SST) was maintained constant during the simulation period using an optimal interpolated SST corresponding to the week prior to when simulation began (Reynolds and Smith, 1994). The hourly outputs of this model were used to force the free surface of the ROMS subdomain in the scenarios that used this atmospheric forcing (Table 1).

Four physical scenarios were generated, each one was simulated for 30 days to study the potential effect of tide and wind as forcings of surface circulation and, as a result, of the areas swept by the viral particles shed by each salmon farm (Table 1). Although the COADS climatology in the study area shows wind blowing predominantly from the west, it presents significant seasonality in the northern component, with predominant wind from the northwest in winter and the southwest in summer. To include this seasonal variation, a scenario was created where the circulation was forced by late-winter climatological wind (September) and another scenario, with mid-summer climatological wind (December). On the other hand, given the time scale over which the ISAv retains its infectious capacity, daily variations in wind also could have the potential to significantly modify the areas swept by the particles. This source of variability was included by generating two more scenarios. One of them was forced with MM5 simulated wind, using synoptic boundary conditions extracted from reanalysis for September, 2008. The other scenario, incorporated synoptic conditions for December 2008. These periods were selected because they included the passing of a strong low pressure system (September scenario) and a high pressure system (December scenario) through the study area.

An evaluation of the nested model was carried out by comparing simulated velocities at 10 m depth with ADCP measurements taken at the same depth, between 2008 and 2009, in 5 mooring sites within the study area (Fig. 2, Table 2). Since no meteorological information associated with these measurements is available, it was not possible to quantify the effect that local wind could have on the surface current. It is expected that daily variations in wind may introduce noise in the simulation that would lead to an

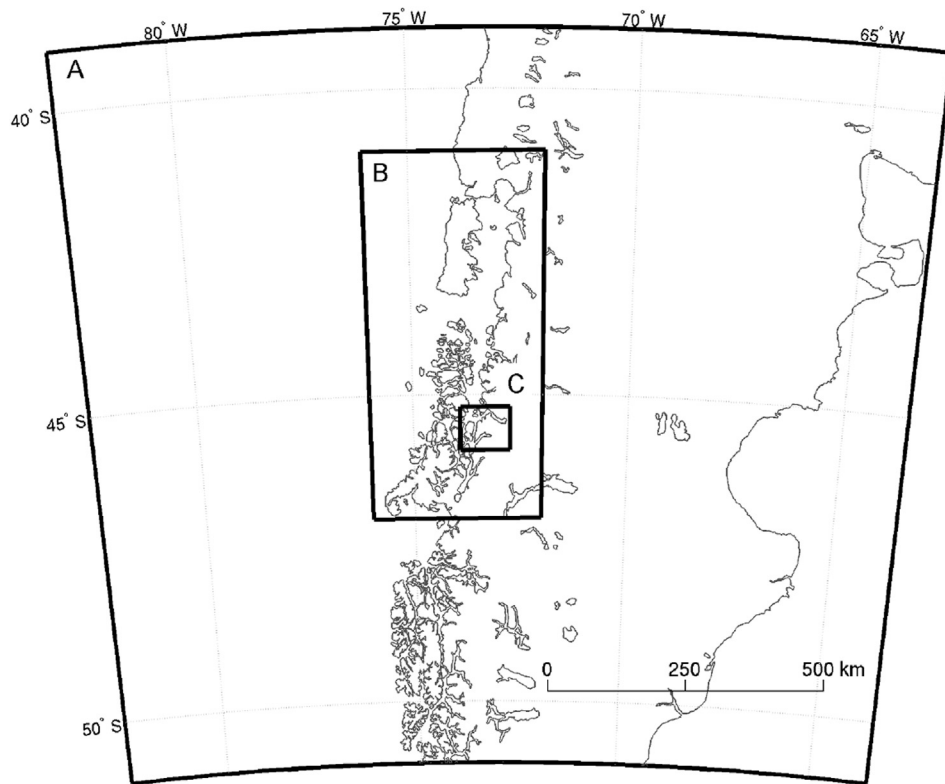


Fig. 1. Simulation domains for the MM5 and ROMS models. (A) domain for the MM5 model. (B) full domain of ROMS and (C) subdomain of ROMS.

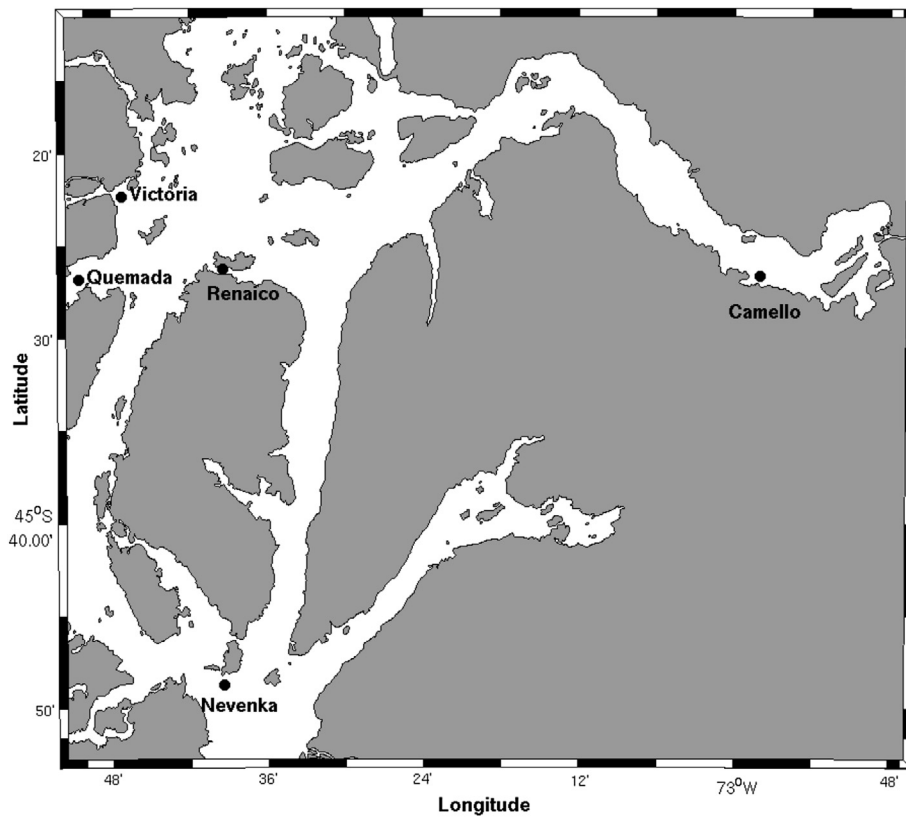


Fig. 2. Geographic localization of current (Victoria: Va, Quemada: Qm, Renaico: Rn, Camello: Cm, Nevenka: Nv) and sea level (Puerto Chacabuco: PCh) observations used to validate the hydrodynamic simulations in the ROMS subdomain.

Table 1
Wind fields used to force the particle dispersions.

Scenario name	Atmospheric forcing
COADS September	COADS climatology for September
COADS December	COADS climatology for December
MM5 September	Simulated MM5. Initialization based on reanalysis for September 2008
MM5 December	Simulated MM5. Initialization based on reanalysis for December 2008

Table 2
Geographic location, sampling period, and depth of ADCP moorings used to validate the hydrodynamic simulations.

Farm	Latitude (S)	Longitude (W)	Sampling period	Moorings depth (m)
Camello	45°27.115'	72°58.731'	08/Apr/09–10/May/09	18
Nevenka	45°48.086'	73°38.400'	10/Jan/09–08/Feb/09	37
Quemada	45°26.237'	73°51.088'	08/Jul/08–06/Aug/08	40
Renaico	45°26.080'	73°38.890'	22/Nov/08–27/Dec/08	21
Victoria	45°22.043'	73°47.119'	06/Apr/09–06/May/09	30

overestimation of the difference between simulations and measurements.

The lagrangian simulations were undertaken using the Ichthyop software (Lett et al., 2008), which uses three-dimensional fields of current, temperature and salinity simulated by ROMS to track both the individual movement of virtual particles and the variables that these particles experience while they are being tracked. In one instantaneous pulse, 100 neutrally buoyant particles were released within the area of each farm (assumed to be 200 × 200 m), randomly distributed in the first 10 m of the water column. Releases were repeated every 2 h over the entire duration of each scenario. Offline particle tracking followed a forward advection scheme. The time interval used to update the position of the particles was 240 s. After being released the particles were tracked up to 24 h according to their previously mentioned 20-h-span activity. After this time the particles were discarded from the simulation. 24 h time frame provides the highest risk from an epidemiological point of view, as we would obtain the highest expected concentration of particles in the areas swept by the simulated condition. Due to the lack of information available in this respect, a decay rate of the virus was also not considered, which also tends to generate maximum risk epidemiological simulations.

The areas swept by the particles released in each farm were based on the proportion of particles present in each ROMS cell with respect to total particles in the water (p_{it}),

$$p_{it} = \frac{n_{it}}{\sum_{i=1}^{nc} n_{it}} \quad (1)$$

where n_{it} is the number of particles in the cell i at time t and nc is the number of cells in the ROMS subdomain. The values for p_{it} were averaged for each cell over the simulation period of the corresponding scenario. The area swept by particles corresponds to that over which this index differs from 0. The value calculated in each case is a proxy for the frequency and/or the density of particles found in the cell.

A risk index for infection was calculated exclusively on the basis of density of particles observed in each swept area. For Atlantic Salmon, Gregory et al. (2009) estimated a maximum rate of ISAV shedding of 42 TCID₅₀ ml⁻¹ kg⁻¹. Because in those experiments the infected fish were maintained for 4 h in a volume of 200 L, without renewal, it can be assumed a total shedding of 8.4 × 10⁶ TCID₅₀ kg⁻¹ in 4 h. Since pulses of particles were released every 2 h in the

simulations, it was assumed that each one was equivalent to 4.2 × 10⁶ TCID₅₀ kg⁻¹. If it is further assumed that the entire biomass of a particular farm is infected, and that this reaches 106 fish of 4 kg, the amount of virus shed in a pulse is 1.68 × 10¹³ TCID₅₀. Accordingly, 1.68 × 10¹¹ TCID₅₀ was assigned to each one of the 100 virtual particles released in one pulse. To obtain the concentration of infectious units, the density of particles in each cell was multiplied first by 1.68 × 10¹¹ TCID₅₀, and then divided by the volume in ml of the first 10 m of one cell. In the study by Gregory et al. (2009), the lowest experimental dose at which infection was produced was 10 TCID₅₀ ml⁻¹. To contrast this figure with the simulated particle densities, a risk field was created taking the maximum TCID₅₀ ml⁻¹ observed in each cell of the ROMS grid over the entire period corresponding to the scenario. Following the results of Gregory et al. (2009), it was considered that infection is highly probable at concentrations equal to, or greater than, 10 TCID₅₀ ml⁻¹, between 10 TCID₅₀ ml⁻¹ and 1 TCID₅₀ ml⁻¹, infection becomes progressively more improbable, and below 1 TCID₅₀ ml⁻¹, infection is not possible.

3. Results

Our simulations show that using the same wind and tidal forcing conditions we can obtain largely different swept areas from salmon farms separated by only a few kilometers. The simulations also show the importance of wind's seasonality on changes in the area swept by the particles (Fig. 4). In farm B, the predominant SW wind in the COADS climatology for December, results in swept areas extending up to 2 km further north than when circulation is forced with the COADS wind of September. Moreover, while the swept area in December does not extend southwards of farm B, the swept area in September does up to 3 km south of the same site. On the other hand, the difference in the area swept by the two climatological wind conditions is greater during neap tide than during spring tide. Therefore, changes in the swept area forced by variations in climatological wind are modulated by variations in the energy of the tidal flows.

The tidal range simulated in the domain with greatest resolution, did not present appreciable geographic variations and was close to 3 m (figure not shown). This value is similar to that measured in Puerto Chacabuco, the only point of the zone where sea level is recorded continuously. The frequency distributions of the simulated velocities underestimated the observed magnitudes (Fig. 3). For example, in the Quemada site (Fig. 3c), 50% of the observations were of a magnitude 0.4 m/s or less, while model results for that area presented 50% of the currents with a magnitude of 0.1 m/s or less. In the rest of the sites the model tends to underestimate velocities when it is forced with wind corresponding to September, and to overestimate when it is forced with wind corresponding to December.

When, in addition to tides, circulation is forced by a relatively stable wind field, simulations show that the area swept by the particles can differ in spring and neap tide. A good example of this is the simulated transport from farm B when is forced by NW wind that dominates the COADS data for September (Fig. 4). In neap tide, the 6 km extension towards SE of the swept area major axis can be explained by wind, while the 3 km over which the minor axis extends can be explained, for the most part, by tidal displacements. On the other hand, even though during spring tide a filament associated to wind blowing towards SE is observed, it does not reach more than 2 km width, while most of the swept area extends over more than 5 km in the NE–SW axis as a result of tidal action. As a consequence, a considerable fraction of the area swept by particles released at farm B during the neap tide is not included in the swept area simulated under spring tide conditions.

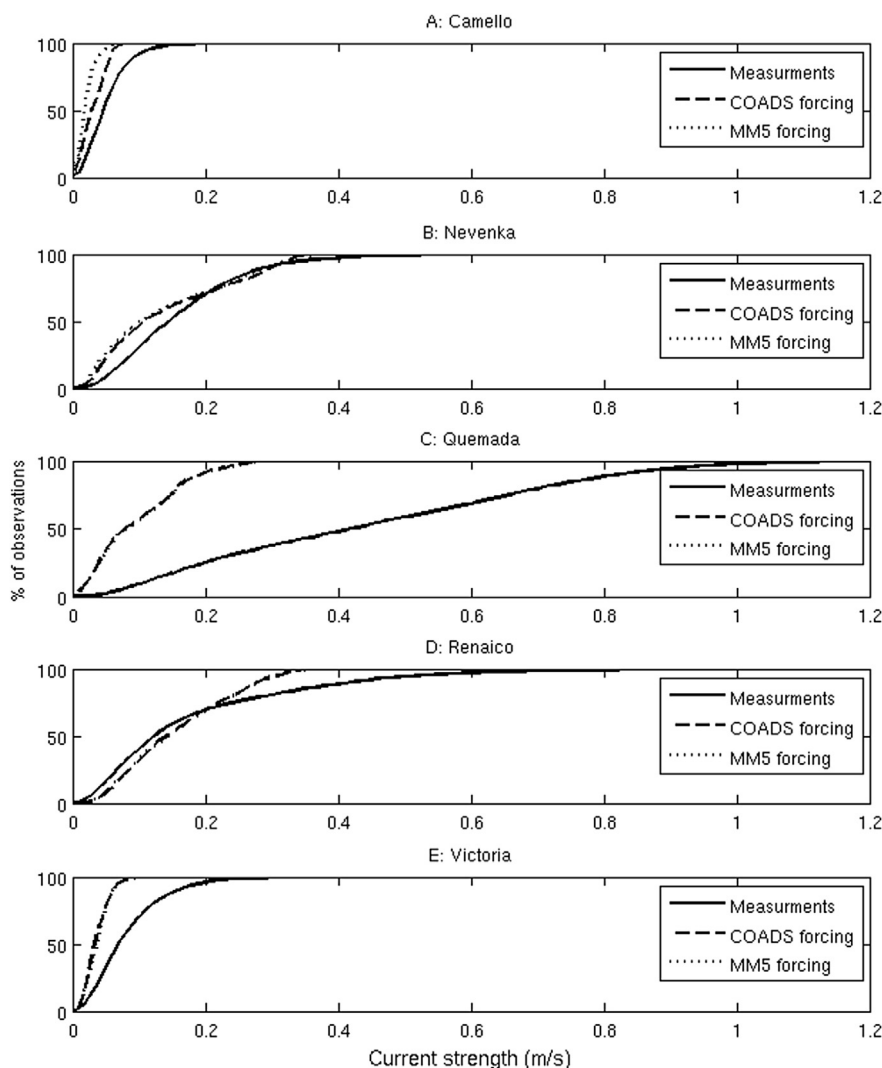


Fig. 3. Cumulative frequency distribution of observed and simulated velocities at 10 m depth in the different sites (Victoria: Va, Quemada: Qm, Renaico: Rn, Camello: Cm, Nevenka: Nv) used to validate the output of the ROMS model.

The extension of swept areas under constant wind forcing can change in different days of fortnightly cycle. Estimates based on only one day (spring or neap tide conditions) can underestimate the area potentially affected by shedding from an infected farm. In fact, the area swept by particles released in B, calculated over a period larger than 15 days (Fig. 5), is greater than the area calculated on the basis of only one day, whether this is a spring tide or a neap tide (Fig. 4). On the other hand, although the swept areas estimated over periods of more than 15 days cover a wider geographic extension, the differences induced by using the climatological September and December wind forcing are equally evident. This highlights the potential of daily wind variations to increase, or at least to modify, the swept areas with respect to those estimated using climatological wind fields.

The purpose of using simulated wind fields to force circulation was to incorporate the inter-daily variation in wind into this forcing, on the assumption that the simulated fields retain the predominance of the NW wind in September and the SW wind in December. Nevertheless, even though the simulated wind field for September showed the tendency observed in climatology (wind from NW), the wind field for December did not, presenting a tendency to blow from the same quadrant as that of September (Fig. 6). This is due to the fact that during December 2008, in addition to the

high atmospheric pressure wave intended to include, a wave of low pressure also affected the region towards the third week of the month, forcing strong winds from the NW. As a result, atmospheric forcings in September and December differed more in the level of their variability than in their average magnitude or direction, with the December 2008 scenario being much more variable than September 2008. The swept area simulated with MM5 for December 2008, was notably greater than the swept area simulated with COADS wind for December, with particles reaching distances more than twice those observed with wind that was stable in time (Fig. 5). In contrast, the area simulated with MM5 for September 2008, although it covers a small fraction of new surface, represents a smaller total area than the swept area simulated with COADS wind for September. This indicates that the reduced temporal variability of the atmospheric forcing found in September 2008, does not increase the variability of the transport, with respect to variability occasioned by the different phases of the fifteen-day tidal cycle.

The evaluation of risks of transmission between farms, requires to consider not only the inter-daily variability of the tidal currents, but also that the forcing by local wind. Although this implies using a temporal series of daily wind fields that is much longer than any of those used in the simulations carried out in this study, we used the

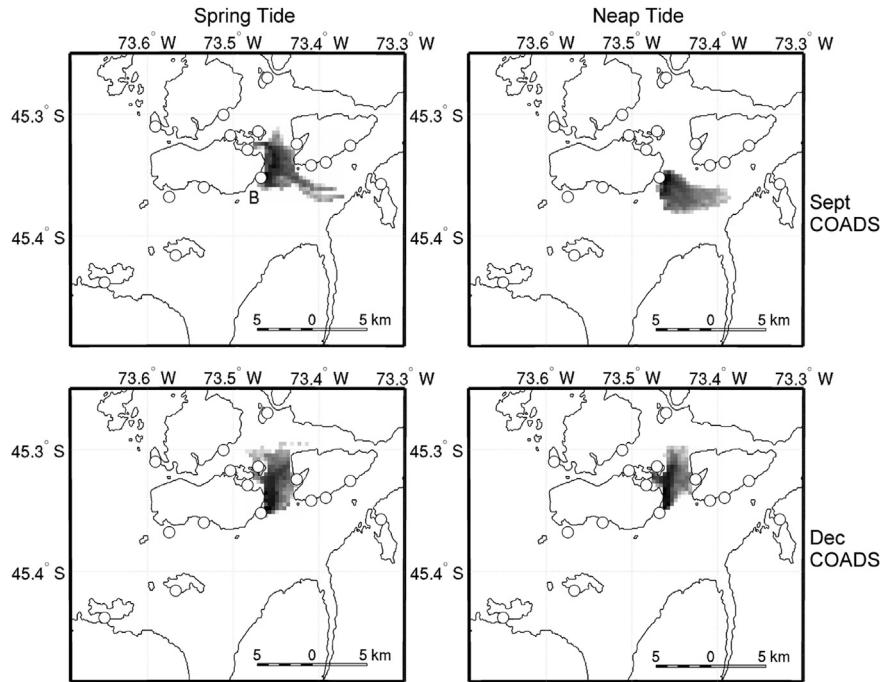


Fig. 4. Area swept over a period of 24 h by the particles released in the farm B during spring tide (left) and neap tide (right), when circulation is forced with COADS climatological wind for September (above) and December (below).

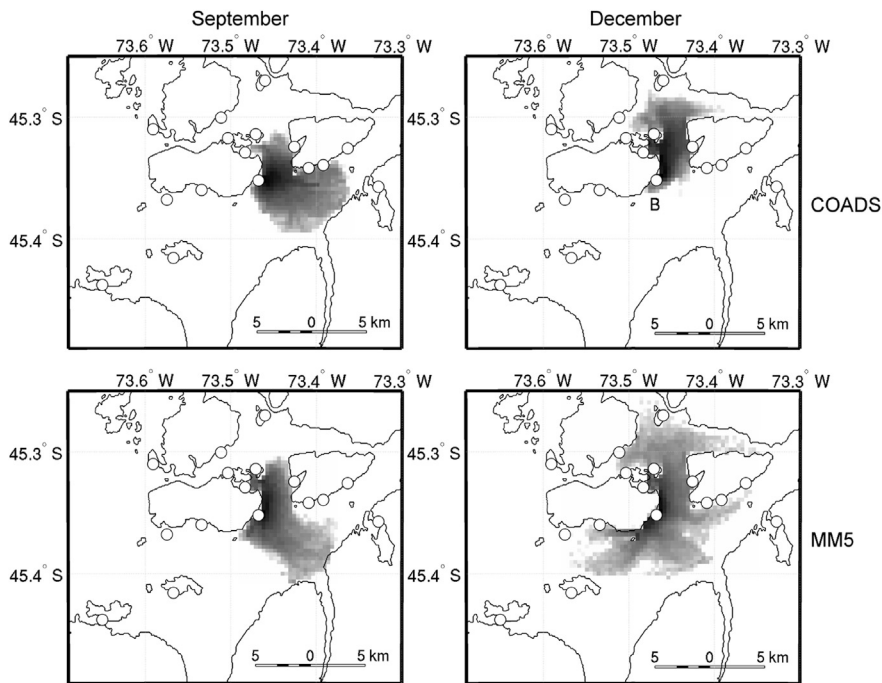


Fig. 5. Area swept by the particles released in farm B over a period of 25 days, when circulation is forced by wind corresponding to September (left) and December (right), taken from the COADS climatology (above) or simulated with MM5 based on reanalysis for 2008 (below).

scenario that integrated greatest wind variability i.e. forced with MM5 wind for December 2008, to produce information for risk assessment. In that scenario (Fig. 7), it is evident that the swept areas of most of the farms reach the position of other farms within the same SMA. This shows that regulatory distance of 2.8 km between farms of the same SMA does not guarantee sanitary isolation, which is not surprising given the assumption that an oceanographic or logistic connection may exist between the farms of the

same SMA. On the other hand, the swept areas (Fig. 7) correspond to farms located at 5.6 km or more from any SMA limit, as established in the present Chilean regulations for isolating one area from another. Nevertheless, farms are observed (A, B, C and F) where their respective swept areas penetrate more than 5.6 km inside another SMA. Furthermore, within the simulated domain, there are farms located at the statutory distance from the limit of their SMA whose swept areas reach 2 neighboring SMA, in both cases beyond

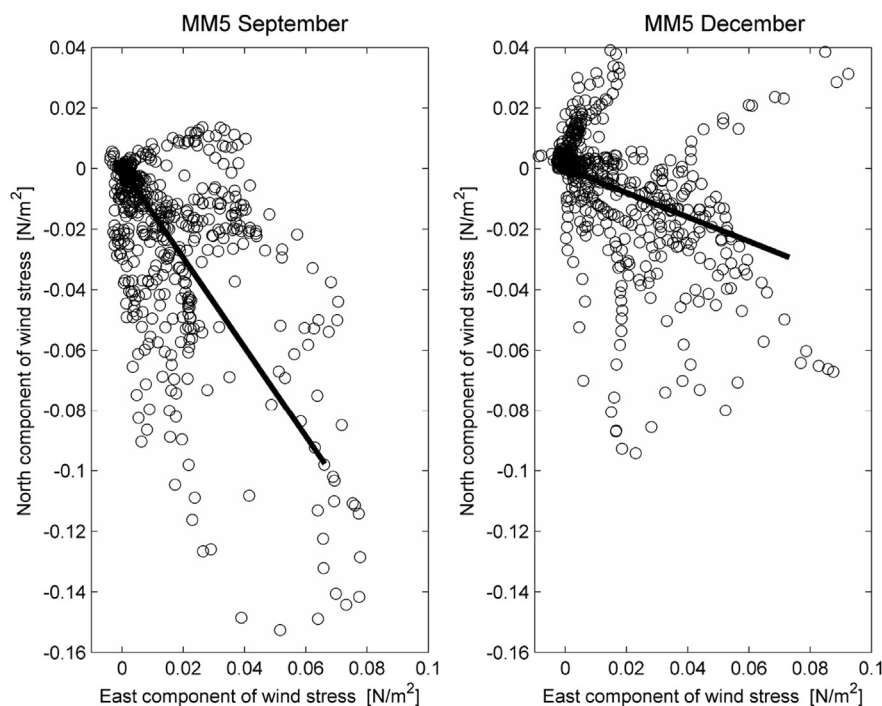


Fig. 6. Distribution of the cartesian components of wind simulated in MM5 for the cell corresponding to the culture center B, during the months of September (left) and December (right), 2008. The line shows the average wind vector multiplied by 5.

5.6 km from their respective limits (F). If we consider the rate at which infected fish shed viral particles into the water, it is possible to estimate the density of viral particles within the area swept by each farm (Fig. 7). In all cases, the area over which viral concentrations are enough to produce infection ($1\text{--}10\text{ TCID ml}^{-1}$) is notably smaller than the area swept by the particles, while the area over which infection is highly probable ($> 10\text{ TCID ml}^{-1}$) is reduced almost to the farm from where the particles originate. Although infection between farms of the same SMA is still probable, the incursion of infectious concentrations into other SMA is reduced, so that only farm F is able to infect a farm 5.6 km away from the limits of another SMA. On the other hand, the wide expanse of the area swept by particles released from farm F, entails a dilution in ISAv concentration in the water, so that (assuming that no farm violates the minimum distance of 5.6 km to any SMA limit) infection between farms in different SMA should not occur in the simulated domain of this study.

4. Discussion

Our simulations show that the same conditions of tide and wind can result in very variable swept areas in farms separated by only a few kilometers. Swept areas tend to be more reduced in the head of the continental fjords (Fig. 7). These geographical differences in ISAv dispersion should be linked to changes in the water velocities, which in turn can be explained by the expected reduction in the amplitude of tidal flows towards the head of the fjords (Aiken, 2008).

The simulations also show that more energetic flow during spring tides promotes a wider dispersion of the ISAv than during the neap tides (Fig. 4). This has been established in previous efforts to estimate both ISAv dispersion (Chang et al., 2005), as well as other viral pathogens (Stucchi et al., 2005). Based on this, it could be argued that an efficient form of estimating the area swept by ISAv involves the use of tidal forcing corresponding only to the spring tide condition. The results obtained in this study indicate

that this is not the case. As other models of marine pathogen dispersion show (Murray and Gillibrand, 2006), our simulations point to the critical influence of wind as a modifier of the transport of pathogens in the ocean. In case the wind direction does not coincide with the major axis of variability in the tidal flows, the resulting transport of particles would sweep different geographical areas in different phases of the fortnightly tidal cycle. From this perspective, although previous studies have calculated dispersion of ISAv on the basis of an average daily tidal cycle (Gustafson et al., 2007b), inclusion of monthly tidal flow variability in estimates of the potential transport of pathogens seems to be necessary.

According to the present simulations, high frequency changes in wind can significantly modify the transport of viral particles from an infected farm. This is indirectly supported by field measurements of wind and current showing the capacity of the wind to modify the circulation in the same zone studied in this research (Cáceres et al., 2002). On one hand, simulations forced with climatological wind point out the need to incorporate seasonal variation into studies on ISAv transmission risk. On the other hand, significant modification of swept areas as a result of inclusion of simulated wind, shows that the daily and inter-daily variability of wind must also be incorporated into risk estimates. To date, the areas swept by marine pathogens have been estimated using wind scenarios either measured *in situ* (Amundrud and Murray, 2009) or simulated (Asplin et al., 2004; Viljugrein et al., 2009). In both cases, however, the scenarios correspond to conditions whose temporal variability is restricted, either by the short time during which wind was measured, or due to idealizations that do not incorporate temporal variability.

Other studies (Asplin et al., 2004, 2014; Johnsen et al., 2014) have pointed to the importance of current generated by baroclinic dynamics in the transport of sea lice in Norway. Recent studies in the Patagonian fjord area (Calvete and Sobarzo, 2011) have described a brackish layer 1–15 m thick, and in particular for the Aysen fjord, where the Camello site (Fig. 2) is located, a short residence time (3.5 d). Residence time of the upper water layer of

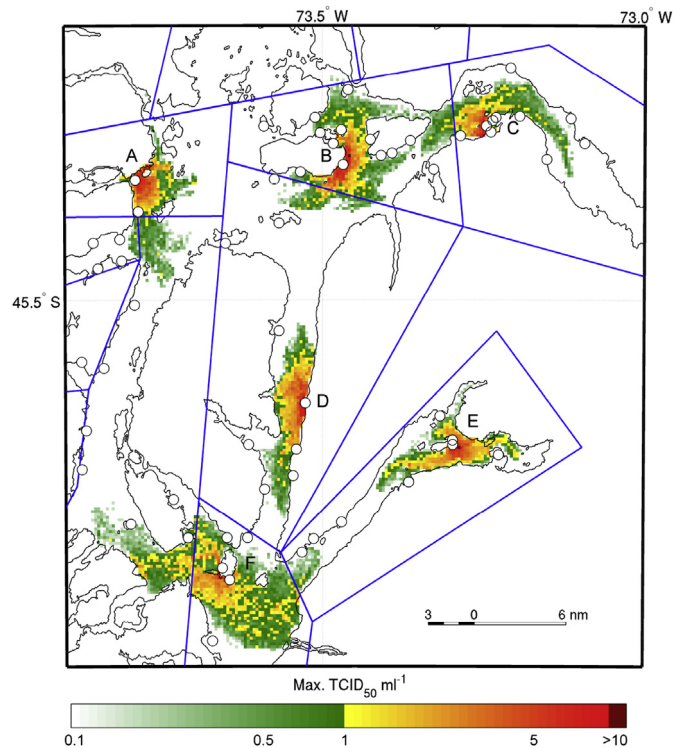


Fig. 7. Swept areas and maximum density ($\text{TCID}_{50} \text{ ml}^{-1}$) reached by viral particles shed in farms located at 5.6 km or more from any SMA limit (marked in blue), when circulation is forced with wind simulated by MM5 for December 2008. (For interpretation of the references to colour in this figure legend, the reader is referred to the web version of this article.)

similar duration (1–2 d) has been related to wind processes in other fjord systems (Asplin et al., 1999). However, as a first step, the stratification of the water column was not considered in this study as we choose to focus on wind and tides, and it will be included in further studies.

The ISAv is expected to remain active in the water column for 20 h, which is relatively shorter than the planktonic stage of the salmon louse is 2–4 weeks (Asplin et al., 2014). Due to this the particles released in these simulations were only tracked for 24 h. In this time frame, the correct representation of episodic events on the current record play a crucial role. The analysis of ADCP records in the Patagonian fjord area shows low frequency residual current (observed minus tidal signal) at several sites (Letelier et al., 2011, Fig. 4d), with residual currents having a continuous positive or negative orientation for 2–3 days, and a magnitude of 0.15 m/s during some events. The use of high resolution atmospheric models could then contribute clarify the importance of wind forcing, particularly the role of high frequency wind events in ISAv dispersion.

The results of this study highlight the need for hydrodynamic models forced with variable wind to generate more realistic risk estimates. Since it is not practical to undertake field campaigns involving simultaneous data collection from numerous sites, over a prolonged period of time, it is probably more efficient to use as forcing for the hydrodynamic model the output of validated, high resolution, atmospheric models, capable of adequately considering the influence of the abrupt topography typical of the fjords (Foreman et al., 2009).

5. Conclusions

We have studied the dispersion of simulated ISAv from salmon farms in the Aysen region. Dispersal patterns were derived from

current fields simulated by the ROMS hydrodynamic model using wind and tide as forcings. Our simulations show that the same forcing conditions can result in largely different swept areas from salmon farms separated by only a few kilometers.

We conclude that the statutory separation between salmon farms defined in Sanitary Management Areas (SMA) do not always generate an effective barrier to ISAv transport by currents. This risk could be reduced if the minimum distance stipulated in the norm is increased. However, the results of this study show that the distance at which ISAv can potentially be transported is highly dependent on geographical location. In the sites where the area swept by particles covers a distance shorter than the current spatial limit, the actual regulation result in unnecessary loss of usable and already scarce space, and a regulatory change that increase the separation between SMAs could result even more detrimental for the industry.

Simulation tools like those used in this study offer a way to improve the role of SMA in preventing ISAv dispersion. By using a validated hydrodynamic model to support the design of SMAs, a regulating agency could acquire the ability to test the outcome of different geographical configurations of salmon farms, being eventually able to generate effective barriers without resorting to a fix distance rule in a given domain.

Acknowledgments

Funding for this study and ancillary measurements in the area were provided by Salmenes FrioSur. Osvaldo E. Arta and Christian Torregrosa assisted with the data analysis. Computing resources were provided by the Geophysics Department, University of Concepcion. HHS was hosted at the Laboratoire de Physique des Océans, Université de Bretagne Occidentale, Brest, France, under the “University of Concepción” Fellowship, while finishing this manuscript. This manuscript was greatly improved by suggestions from one anonymous reviewer and observations by Dr. Lars Asplin, whose interest and contributions to this topic we appreciate.

References

- Aiken, C., 2008. Barotropic tides of the Chilean Inland Sea and their sensitivity to basin geometry. *J. Geophys. Res.* C113, 1–13.
- Aldrin, M., Storvik, B., Frigessi, A., Viljugrein, H., Jansen, P.A., 2010. A stochastic model for the assessment of the transmission pathways of heart and skeleton muscle inflammation, pancreas disease and infectious salmon anaemia in marine fish farms in Norway. *Prev. Veterinary Med.* 93, 51–61.
- Amundrud, T.L., Murray, A.G., 2009. Modelling sea lice dispersion under varying environmental forcing in a Scottish sea loch. *J. Fish Dis.* 32, 27–44.
- Asplin, L., Salvanes, A.G.V., Kristoffersen, J.B., 1999. Nonlocal winddriven fjordcoast advection and its potential effect on plankton and fish recruitment. *Fish. Oceanogr.* 8, 255–263.
- Asplin, L., Boxaspen, K., Sandvick, A.D., 2004. Modelled distribution of salmon lice in a Norwegian fjord. *ICES J. Mar. Sci.* 1–12. CM 2004/P:11.
- Asplin, L., Johnsen, I.A., Sandvik, A.D., Albretsen, J., Sundfjord, V., Aure, J., Boxaspen, K.K., 2014. Dispersion of salmon lice in the Hardangerfjord. *Mar. Biol.* Res. 10 (3), 216–225. <http://dx.doi.org/10.1080/17451000.2013.810755>.
- Cáceres, M., Valle-Levinson, A., Sepúlveda, H.H., Holderied, K., 2002. Transverse variability of flow and density in a Chilean fjord. *Cont. Shelf Res.* 22, 1683–1698.
- Calvete, C., Sobarzo, M., 2011. Quantification of the surface brackish water layer and frontal zones in southern Chilean fjords between Boca del Guafo (43° 30'S) and Estero Elefantes (46° 30' S. *Cont. Shelf Res.* 31 (3–4), 162–171.
- Chang, B.D., Page, F.H., Losier, R.J., Greenberg, D.A., Chaffey, J.D., McCurdy, E.P., 2005. Application of a tidal circulation model for fish health management of salmon farms in the Grand Manan Island Area, Bay of Fundy. *Bull. Aquac. Assoc. Can.* 105, 22–33.
- Conkright, M.E., Locarnini, R.A., Garcia, H.E., O'Brien, T.D., Boyer, T.P., Stephens, C., Antonov, J., 2002. World Ocean Atlas 2001: Objectives, Analyses, Data Statistics and Figures [D-ROM]. NOAA Atlas NESDIS 42, Silver Spring, MD.
- Da Silva, A.M., Young, C.C., Levitus, S., 1994. Atlas of Surface Marine Data. In: Algorithms and Procedures, vol. 1. NOAA, Silver Spring, MD. Tech Report.
- Dudhia, J., 1993. A nonhydrostatic version of the Penn State-NCAR mesoscale model: validation tests and simulation of an Atlantic cyclone and cold front. *Mon. Weather Rev.* 121, 1493–1513.

- Dudhia, J., 1989. Numerical study of convection observed during the Winter Monsoon Experiment using a mesoscale two-dimensional model. *J. Atmos. Sci.* 46, 3077–3107.
- Egbert, G., Erofeeva, S., 2002. Efficient inverse modeling of barotropic ocean tides. *J. Atmos. Ocean. Technol.* 19, 183–204.
- Foreman, M.G., Czajko, P., Stucchi, D.J., Guo, M., 2009. A finite volume model simulation for the Broughton Archipelago, Canada. *Ocean. Model.* 30, 29–47.
- Gregory, A., Munro, L.A., Snow, M., Urquhart, K.L., Murray, A.G., Raynard, R.S., 2009. An experimental investigation on aspects of infectious salmon anaemia virus (ISAV) infection dynamics in seawater Atlantic Salmon, *Salmo salar* L. *J. Fish Dis.* 32, 481–489.
- Grell, G., 1993. Prognostic evaluation of assumptions used by cumulus parametrizations. *Mon. Weather Rev.* 121, 764–787.
- Gustafson, L., Ellis, S., Robinson, T., Marengi, F., Merrill, P., Hawkins, L., Giray, C., Wagner, B., 2007a. Spatial and non-spatial risk factors associated with cage-level distribution of infectious salmon anaemia at three Atlantic Salmon, *Salmo salar* L., farms in Maine, USA. *J. Fish Dis.* 30, 101–109.
- Gustafson, L.L., Ellis, S.K., Beattie, M.J., Chang, B.D., Dickey, D.A., Robinson, T.L., Marengi, F.P., Moffett, P.J., Page, F.H., 2007b. Hydrographics and the timing of infectious salmon anaemia outbreaks among Atlantic Salmon (*Salmo salar* L.) farms in the Quoddy region of Maine, USA and New Brunswick, Canada. *Prev. Veterinary Med.* 78, 35–56.
- IOC, IHO, BODC, 2003. Centenary Edition of the GEBCO Digital Atlas, Published on CD-ROM on Behalf of the Intergovernmental Oceanographic Commission and the International Hydrographic Organization as Part of the General Bathymetric Chart of the Oceans. British Oceanographic Data Centre, Liverpool, U.K.
- Jarp, J., Karlsen, E., 1997. Infectious salmon anemia (ISA) risk-factors in sea-cultured Atlantic Salmon *Salmo salar*. *Dis. Aquat. Org.* 28, 79–86.
- Johnsen, I.A., Fiksen, Ø., Sandvik, A.D., Asplin, L., 2014. Vertical salmon lice behaviour as a response to environmental conditions and its influence on regional dispersion in a fjord system. *Aquac. Environ. Interact.* 5, 127141. <http://dx.doi.org/10.3354/aei00098>.
- Kalnay, E., Kanamitsu, M., Kistler, R., Collins, W., Deaven, D., Gandin, L., Iredell, M., Saha, S., White, G., Woollen, J., Zhu, Y., Leetmaa, A., Reynolds, R., Chelliah, M., Ebisuzaki, W., Higgins, W., Janowiak, J., Mo, K.C., Ropelewski, C., Wang, J., Jenne, R., Joseph, D., 1996. The NCEP/NCAR 40-Year reanalysis project. *Bull. Am. Meteorol. Soc.* 77 (3), 437–471. <http://dx.doi.org/10.1175/1520-0477>.
- Katz, J., Iizuka, M., Muñoz, S., 2011. Creciendo en base a los recursos naturales, "tragedias de los comunes" y el futuro de la industria salmonera chilena. In: *Serie Desarrollo Productivo*, vol. 191. CEPAL (UN), Santiago de Chile.
- Kibenge, F.S.B., Godoy, M.G., Wang, Y., Kibenge, M.J.T., Gherardelli, V., Mansilla, S., Lisperger, A., Jarpa, M., Larroquette, G., Avendaño, F., Lara, M., Gallardo, A., 2009. Infectious salmon anaemia virus (ISAV) isolated from the ISA disease outbreaks in Chile diverged from ISAV isolates from Norway around 1996 and was disseminated around 2005, based on surface glycoprotein gene sequences. *Virol. J.* 6, 88.
- Letelier, J., Soto-Mardones, L., Salinas, S., Osuna, P., López, D., Sepúlveda, H.H., Pinilla, E., Rodrigo, C., 2011. Variability of wind, waves and currents in the north Chilean Patagonic fiords. *Rev. Biol. Mar. Oceanogr.* 46 (3), 363–377.
- Lett, C., Verley, P., Mullon, C., Parada, C., Brochier, T., Penven, P., Blanke, B., 2008. A Lagrangian tool for modelling ichthyoplankton dynamics. *Environ. Model. Softw.* 23, 1210–1214.
- Lyngstad, T.M., Jansen, P.A., Sindre, H., Jonassen, C.M., Hjortaa, M.J., Johnsen, S., Brun, E., 2008. Epidemiological investigation of infectious salmon anaemia (ISA) outbreaks in Norway 2003–2005. *Prev. Veterinary Med.* 84, 213–227.
- Mason, E., Molemaker, J., Shchepetkin, A.F., Colas, F., McWilliams, J.C., Sangra, P., 2010. Procedures for offline grid nesting in regional ocean models. *Ocean. Model.* 35, 1–15.
- Mikalsen, A.B., Teig, A., Helleman, A., Mjaaland, S., Rimstad, E., 2001. Detection of infectious salmon anaemia virus (ISAV) by RT-PCR after cohabitant exposure in Atlantic Salmon *Salmo salar*. *Dis. Aquat. Org.* 47, 175–181.
- Mjaaland, S., Markussen, T., Sindre, H., Kjøglum, S., Dannevig, B.H., Larsen, S., Grimholt, U., 2005. Susceptibility and immune responses following experimental infection of MHC compatible Atlantic Salmon (*Salmo salar* L.) with different infectious salmon anaemia virus isolates. *Arch. Virol.* 150, 2195–2216.
- Murray, A.G., Smith, R.J., Stagg, R.M., 2002. Shipping and the spread of infectious salmon anaemia in Scottish aquaculture. *Emerg. Infect. Dis.* 8, 1–5.
- Murray, A.G., Gillibrand, P.A., 2006. Modelling salmon lice dispersal in Loch Torridon, Scotland. *Mar. Pollut. Bull.* 53, 128–135.
- Nylund, A., Hovland, T., Hodneland, K., Nilsen, F., Levik, P., 1994. Mechanisms for transmission of infectious salmon anaemia (ISA). *Dis. Aquat. Org.* 19, 95–100.
- Penven, P., Echevin, J., Pasapera, J., Colas, F., Tam, J., 2005. Average circulation, seasonal cycle, and mesoscale dynamics of the Peru current System: a modeling approach. *J. Geophys. Res.* C110, C10021. <http://dx.doi.org/10.1029/2005JC002945>.
- Raynard, R.S., Murray, A.G., Gregory, A., 2001. Infectious salmon anaemia virus in wild fish from Scotland. *Dis. Aquat. Org.* 46, 93–100.
- Reynolds, R.W., Smith, T.M., 1994. Improved global sea surface temperature analysis using optimal interpolation. *J. Clim.* 6, 768–774.
- Ritchie, R.J., Cook, M., Melville, K., Simard, N., Cusack, R., Griffiths, S., 2001. Identification of infectious salmon anaemia virus in Atlantic Salmon from Nova Scotia (Canada): evidence for functional strain differences. *Dis. Aquat. Org.* 44, 171–178.
- Ritchie, R.J., McDonald, J.T., Glebe, B., Young-Lai, W., Johnsen, E., Gagna, N., 2009. Comparative virulence of infectious salmon anaemia virus isolates in Atlantic Salmon, *Salmo salar* L. *J. Fish Dis.* 32, 157–171.
- Shchepetkin, A.F., McWilliams, J.C., 2005. The regional oceanic modeling system (ROMS): a split-explicit, free-surface, topography-following-coordinate oceanic model. *Ocean. Model.* 9, 347–404.
- Scheel, I., Aldrin, M., Frigessi, A., Jansen, P.A., 2007. A stochastic model for infectious salmon anaemia (ISA) in Atlantic Salmon farming. *J. R. Soc. Interface* 4, 699–706.
- Stucchi, D.J., Henry, R.F., Foreman, M.G.G., 2005. Modelling the transport and dispersion of IHN pathogens in the Broughton Archipelago, British Columbia. *Bull. Aquac. Assoc. Can.* 105 (1), 52–59.
- Totland, G.K., Hjeltne, B.K., Flood, P.R., 1996. Transmission of infectious salmon anaemia (ISA) through natural secretions and excretions from infected smolts of Atlantic Salmon *Salmo salar* during their presymptomatic phase. *Dis. Aquat. Org.* 26, 25–31.
- Troen, I., Mahrt, L., 1986. A simple model of the atmospheric boundary layer: sensitivity to surface evaporation. *Boundary-Layer Meteorol.* 37, 129–148.
- Vike, S., Nylund, S., Nylund, A., 2009. ISA virus in Chile: evidence of vertical transmission. *Arch. Virol.* 154, 1–8.
- Viljugrein, H., Staalstrøm, A., Molvær, J., Urke, H.A., Jansen, P.A., 2009. Integration of hydrodynamics into a statistical model on the spread of pancreas disease (PD) in salmon farming. *Dis. Aquat. Org.* 88, 35–44.